Наносистеми, наноматеріали, нанотехнології
Nanosistemi, Nanomateriali, Nanotehnologii
2021, т. 19, № 1, сс. 53–70

© 2021 ІМФ (Інститут металофізики
ім. Г. В. Курдюмова НАН України)
Надруковано в Україні.

PACS numbers: 07.07.Df, 68.37.Hk, 68.55.J-, 81.07.-b, 81.15.Gh, 81.20.Ka, 82.47.Rs

Electrical Properties and Sensitivity of SnO_2 Nanostructures to Organic Compounds

T. Yashchenko[1], A. Sviderskyi[1], S. Nahirniak[1], T. Dontsova[1], and S. Kalinowski[2]

[1]*National Technical University of Ukraine 'Igor Sikorsky Kyiv Polytechnic Institute', 37, Peremogy Ave., UA-03056 Kyiv, Ukraine*
[2]*Department of Chemistry, Uniwersytet Warmińsko-Mazurski w Olsztynie, ul. Michała Oczapowskiego 2, PL-10-719 Olsztyn, Polska*

Metal-oxide semiconductors are the most widely used gas-sensitive materials due to their numerous advantages such as high sensitivity to various gases with ease of production, high compatibility with other processes, low cost, simplicity of measurements along with minimal energy consumption. From this point of view, investigations of the morphological and electrical characteristics of metal-oxide materials, particularly based on tin(IV) oxide, and the determination of their sensitivity to organic compounds such as ethyl acetate and chlorobenzene are extremely important. In this work, tin(IV)-oxide nanostructures have been synthesized by chemical vapour deposition (CVD) technique and modified with argentum. Obtained samples have been investigated with electron microscopy, and as a result, it was found that, during the synthesis under different conditions, nanoparticles of zero- and mixed zero- and one-dimensional morphology were obtained. The study of electrical characteristics and sensitivity towards vapours of ethyl acetate and chlorobenzene has been carried out. The comparison of electrical properties and sensitivity to the vapours of organic substances of pure and modified $0D$- and mix $0D + 1D$-SnO_2-samples is presented. It was found that morphology affects not only electrical properties of tin(IV)-oxide nanostructures, but also their sensing properties. It was shown that the addition of argentum has an ambiguous effect on the sensitivity depending on the morphology of the obtained samples; modification leads to increasing of $0D$-sample sensitivity and decreasing of sensing response for $0D + 1D$-SnO_2-sample.

Напівпровідники з металооксиду є найбільш широко використовувани-

ми газочутливими матеріялами завдяки їхнім численним перевагам, таким як висока чутливість до різних газів при простоті виробництва, висока сумісність з іншими процесами, низька вартість, простота мірянь поряд з мінімальними енерговитратами. З цієї точки зору дослідження морфологічних та електричних характеристик металооксидних матеріялів, особливо на основі оксиду олива(IV), та визначення їхньої чутливости до органічних сполук, таких як етилацетат і хлорбензол, надзвичайно важливі. У цій роботі наноструктури оксиду олива(IV) синтезовані методою хемічного парового осадження та модифіковані Арґентумом. Одержані зразки досліджували за допомогою електронної мікроскопії, і в результаті було встановлено, що під час синтези в різних умовах були одержані наночастинки нульової та змішаної нульової й одновимірної морфології. Проведено дослідження електричних характеристик і чутливости до пар етилацетату та хлорбензолу. Представлено порівняння електричних властивостей і чутливости до пар органічних речовин чистих і модифікованих $0D$- та суміші $0D + 1D$-SnO_2 зразків. Встановлено, що морфологія впливає не тільки на електричні властивості наноструктур оксиду олива(IV), а й на їхні чутливі властивості. Показано, що додавання Арґентуму має неоднозначний вплив на чутливість залежно від морфології одержаних зразків; модифікування приводить до збільшення чутливости $0D$-зразка та зменшення чутливости реакції для $0D + 1D$-SnO_2-зразка.

Key words: SnO_2 nanostructures, morphology, modification with argentum, electrical properties, sensitivity, volatile organic compound.

Ключові слова: наноструктури SnO_2, морфологія, модифікація Арґентумом, електричні властивості, чутливість, летка органічна сполука.

(Received 16 April, 2020)

1. INTRODUCTION

The development of sensors for the identification of volatile organic compound (VOC) vapours is relevant in connection with the intensive development of industrial processes such as oil refining, petrochemical production and construction [1–4]. It is known that VOCs are one of the main causes of air pollution, and almost all of them are flammable. Currently, the level of VOCs emissions has become a serious problem all over the world and some of them can cause direct harm to human health [5], the prominent representatives of which are ethyl acetate and chlorobenzene vapours.

Ethyl acetate ($CH_3COOC_2H_5$) belongs to the IV hazard class. Ethyl acetate gives occasion to irritation of skin (dryness and formation of cracks), prolonged inhalation may cause damage of kidneys and liver, irritates the mucous membranes of the eye and respiratory tract. It is toxic to the nervous system. Ethyl acetate has low level

of volatility. Its chemical properties are similar to those of acetone, so working with it necessitates caution [6]. Chlorobenzene (C_6H_5Cl) belongs to the III hazard class and causes localized redness, swelling, itching, and problems of the gastrointestinal tract, headache and dizziness. Chlorobenzene is explosive and toxic [7].

Thermocatalytic, IR absorption, electrochemical (amperometric), photoionization, and semiconductor sensors are especially noted among gas sensors used to determine VOCs due to their compactness, mobility, and fast reaction [8–11]. Among listed sensors, metal-oxide conductometric gas sensors are of great interest in the gas environment quality control due to high sensitivity, ease of production, low cost, ease of use and minimal energy consumption [12, 13]. One of the main characteristics that determine the field of semiconductor gas sensors application is response sensitivity. The sensor sensitivity directly depends on the properties of the sensitive material. That is why chemical and structural characteristics such as morphology, particle size, specific surface area, chemical composition, and defects of the material are considered [14, 15].

It is known that morphology of metal oxides particles significantly affects their electrical properties [16]. In [17], a comparative study of the electrical characteristics of round-shaped and thread-like SnO_2 nanoparticles obtained by same synthesis method was carried out. As a result, it was shown that morphology significantly affects their electrical characteristics: the current–voltage dependences vary from characteristic for semiconductor (for rounded nanoparticles) to ohmic (for thread-like nanoparticles) materials. The electrical properties of metal oxides are also significantly affected by their chemical composition and defects [18, 19]. In addition, in [20–22], it was shown that a decrease in the particle size and an increase in the specific surface lead to improvement in sensitivity to many vapours and gases.

Tin(IV) oxide is the most promising sensing material among a wide set of semiconducting metal oxides [4, 23, 24]. However, sensory materials based on pure SnO_2 also have certain disadvantages, which include lack of sensitivity for some applications, low selectivity and poor stability [25–27]. To eliminate these shortcomings, doping, modification and composite creation on the base of pure SnO_2 are used [28–33]. To increase the sensitivity of tin(IV)-oxide layers to VOCs, modifiers such as noble metals (Pt, Pd, Au), metal oxides (Co_3O_4, In_2O_3, ZnO, *etc.*) and carbon nanomaterials are mainly used [34, 35]. It should be noted that in the literature there is no information on usage such modifier as argentums, which is an order of magnitude cheaper than noble metals.

The goal of this paper is to investigate the influence of morphology and argentum modification on the electrical properties and sen-

sitivity of tin(IV)-oxide nanostructures towards vapours of organic substances such as ethyl acetate and chlorobenzene.

2. EXPERIMENTAL TECHNIQUE

2.1. Materials Synthesis

SnO_2 nanostructures of different morphology (round-shaped and wire-like) were synthesized by chemical vapour deposition (CVD) technique from tin(II) oxalate in the inert nitrogen atmosphere [36, 37]. Formation of tin(IV) nanostructures of different morphology was achieved by varying the process parameters, namely the temperature, precursor, heating rate and synthesis duration [38]. A study of the effects of CVD synthesis conditions showed that the structure and morphology of SnO_2 essentially depend on the type of precursor and the heating rate and slightly on the synthesis temperature. It was established that reducing the heating rate from 80 deg/min to 20 deg/min changes the morphology of tin(IV) oxide from nanosize to one-dimensional nanostructures.

The modified SnO_2 samples were obtained by impregnating obtained tin(IV) oxide powders with the argentum(I) nitrate solution with subsequent thermal decomposition [39]. For this, the calculated volume of the $AgNO_3$ solution was added to the 0.2 g of SnO_2. The resulting suspension was poured with 1 cm^3 of double distilled water and left for 7 days. The samples were further dried at 383 K for 1 hour and calcined at 673 K for 2 hours.

2.2. Characterization Techniques

To study electrical properties of the obtained pure and modified tin(IV)-oxide materials, the sensitive layer was formed according to [40] by the method of coating by drop. Obtaining the film on the substrate was carried out as follows. First, the substrate was cleaned with ethyl alcohol in an ultrasound bath for 2–3 minutes and then fixed in a centrifuge. At the same time, the suspension of the powder at issue with organic solvent (1,2-propanediol) was prepared. The drop of the prepared suspension was applied to the centre of the substrate and centrifuged at the speed of 6200 rpm for 2 minutes to form the continuous layer. The procedure was repeated 3 times. After this, the substrate with obtained layer was dried at 200°C for 15 minutes.

Figure 1 shows the electrical scheme of the experimental setup for electrical properties investigation. The potentiostat/galvanostat DPTG-317 [41] was guided by the program that allows registration

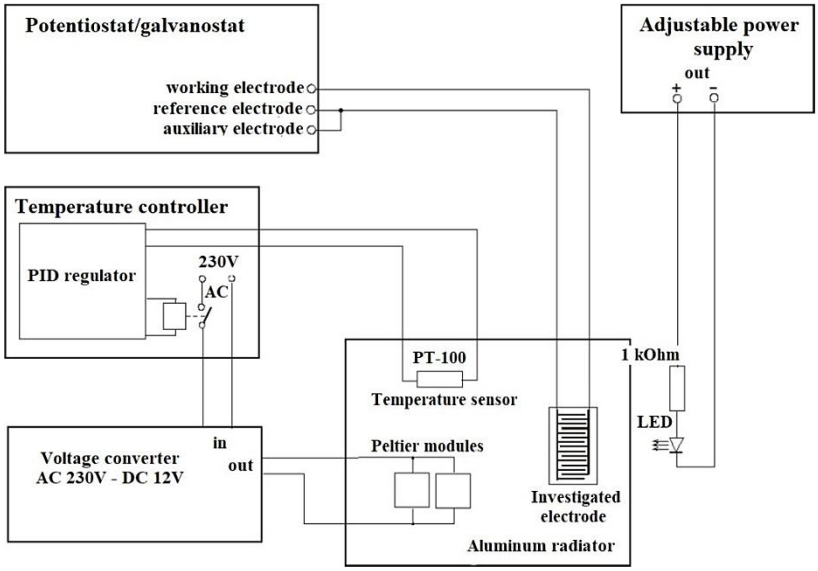

Fig. 1. Electrical scheme of the experimental setup.

of voltammetric, chronoamperometric and other curves. At the same time, this device also facilitates current analysis. The applied electrode potential varied in the range of ±5 V.

Heating to 423 K and cooling of the electrode was carried out using two Peltier modules that were connected to the temperature controller REX C-100. When cooling, the voltage was applied in the opposite direction. The practically achieved cooling of the investigated substrate was 283 K. The substrate holder with the layer of the investigated SnO_2 powder was attached from the top to the Peltier module. The Peltier module was connected to the radiator for transferring heat either way. To achieve the minimum temperature, the fan was used to blow at the aluminium radiator.

Almost all of studied powders showed resistance higher than 1 MOhm that means the currents passing through the electrodes are very small, usually less than 0.1 μA. Such systems are vulnerable to external noise, so the electrodes and wires had to be screened. For this purpose, the aluminium holder closed from above by the aluminium electrode shield was made. Additionally, the body contained the hole for supplying analyzed gases.

The system also included the power supply RXN-1505D with adjustable output voltage from 0 to 15 V. The maximum thermal efficiency was 5 A. The potentiostat/galvanostat was connected to the PC and all measurements were recorded using the 'Cyclic voltammetry' program [41] As a result, the voltamperometric curve with the

values of the applied voltage on the X-axis (varied linearly in the specified range) and the current intensity on the Y-axis was obtained. From the obtained curve in different sections of the graph (at specific points of the curve), the resistance of the electrode was determined. The resistance was calculated using the least squares method. If the obtained dependence was nonlinear, the applied voltage influenced the resistance of this material.

The device is intended for electrochemical tests and is modular in structure. The device interacts with the computer through the LPT connector, providing the parallel, fast transfer of 8-bit data. The potentiostat/galvanostat KSP is intended for use in systems requiring very high sensitivity and low noise levels. The software for the measurements control was written in Delphi.

To study electrical properties of SnO_2 samples in the atmosphere of studied gas, the gas medium was created. For this purpose, 2–5 cm^3 of the organic liquid was collected using the special 20 cm^3 syringe, after which the syringe was pumped with air at the certain temperature. After that, the remaining liquid was poured out and the resulting gas was blended to 20 cm^3, and thus, the gas concentration of 25% was achieved. To calculate the pressure of saturated vapours of organic substances, the Antoine equation was used [42].

3. RESULTS AND DISCUSSION

3.1. Samples

The varying of process conditions during CVD synthesis led to the

TABLE 1. Obtained pure and modified SnO_2 samples.

Sample	Description
$0D$-SnO_2	Zero-dimensional tin(IV) oxide nanostructures synthesized at heating rate 80 deg/min
$0D + 1D$-mix SnO_2	Mix of zero- and one-dimensional tin(IV) oxide nanostructures synthesized at heating rate 20 deg/min
$0D$-2AgSnO_2	$0D$-SnO_2 sample modified with 2% of argentum
$0D$-5AgSnO_2	$0D$-SnO_2 sample modified with 5% of argentum
$0D$-10AgSnO_2	$0D$-SnO_2 sample modified with 10% of argentum
$0D + 1D$-mix 2AgSnO_2	$0D + 1D$-mix SnO_2 sample modified with 2% of argentum
$0D + 1D$-mix 5AgSnO_2	$0D + 1D$-mix SnO_2 sample modified with 5% of argentum
$0D + 1D$-mix 10AgSnO_2	$0D + 1D$-mix SnO_2 sample modified with 10% of argentum

establishment that reducing the heating rate of the furnace from 80 deg/min to 20 deg/min changes the morphology of tin(IV) oxide from nanosize to one-dimensional nanostructures. Thus, two tin(IV) oxide samples were obtained: zero-dimensional structures synthesized at 80 K/min, the faster heating rate; mixed zero- and one-dimensional SnO_2 nanostructures synthesized at the same synthesis conditions but using 20 K/min, the slower heating rate. Obtained samples were modified with argentum in amounts of 2%, 5% and 10%. Obtained tin(IV)-oxide samples are presented in Table 1.

3.2. SEM Results

SEM microphotographs of unmodified and modified SnO_2 samples processed using Quanta FEG 250 at two different heating rates are shown in Fig. 2.

$0D$-SnO_2 sample synthesized at 80 K/min fast heating rate has a dense porous structure with predominant grain size of 1–2 microns and characterized by formation of particles of uneven and needle shapes. $0D + 1D$-mix SnO_2 sample obtained with the reduced heating rate of 20 deg/min is the mixture of the fine and coarse-disperse needle-shaped powder. Thus, it can be seen that different synthesis conditions, namely the speed of the heating rate, causes the change of tin(IV)-oxide morphology and allows to obtain one-dimensional SnO_2 nanoneedles.

As one can see from the presented images of modified zero-dimensional and mixed zero- and one-dimensional SnO_2 samples, in the case of $0D$-SnO_2 sample, as the content of the argentum grows, the number of agglomerates increases. From the data of the electron microscopy for the modified mixed $0D + 1D$-mix SnO_2 samples, it is evident that the needle form predominates in the tin(IV)-oxide sample doped with argentum in the amount of 5%, while with the argentum content of 10%, there is a presence of larger pieces of the metal itself.

3.3. Current–Voltage Dependences

Electrical characteristics of the SnO_2 powders were studied using the cyclic voltammetry technique. The current range was selected automatically, depending on the current values set in the graphic field. At any moment, the registration of current could be stopped, or the direction of potential sweep could be changed. This program was used to determine the current–potential characteristics of the tested powders, and to calculate the resistance or conductivity values on their basis. The program allowed investigating the stability

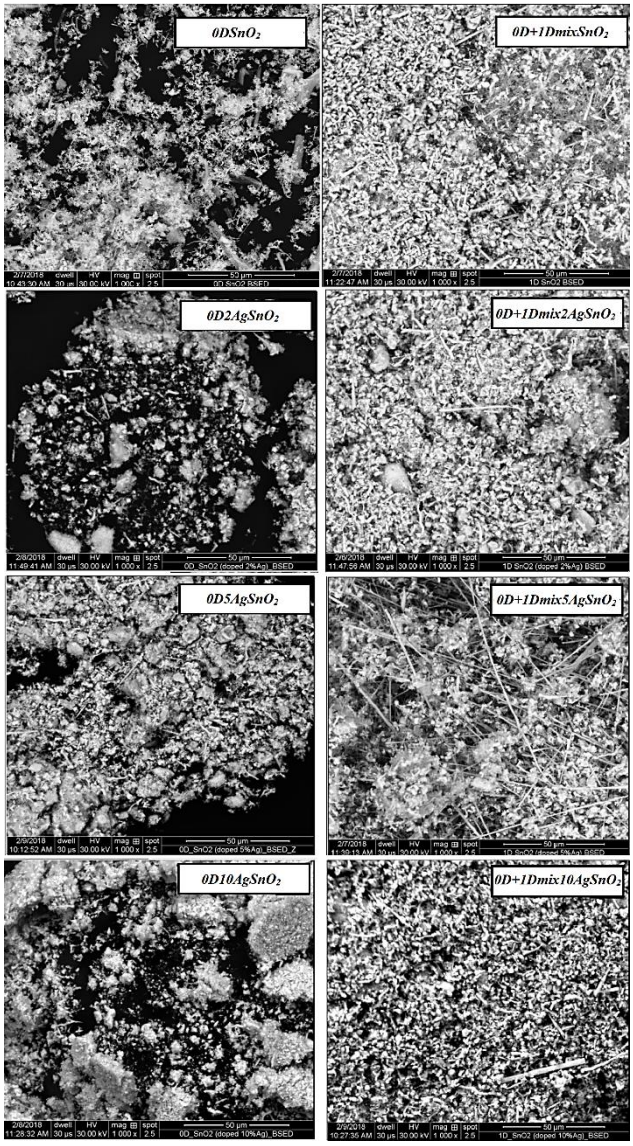

Fig. 2. SEM images of SnO_2 samples.

of the studied systems under influence of time, temperature and photoelectric effects.

Cyclic voltammograms of all samples at ambient are shown in Fig. 3. For all samples, there is a change in resistance, depending on the applied voltage, which is the characteristic of materials with semiconductor properties. Cyclic voltammetry curves for synthe-

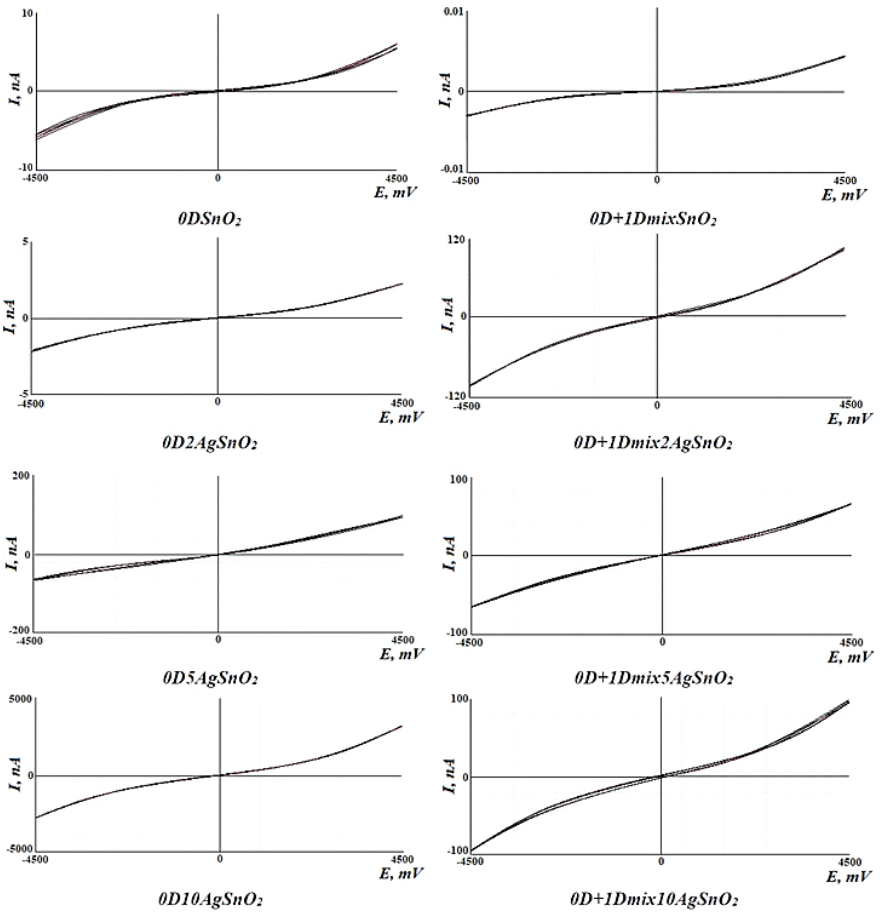

Fig. 3. *I*–*U* curves of SnO_2 samples.

sized samples differ not only in appearance (presence or absence of hysteresis), but also in magnitude of current flowing through the substrate.

Unlike the mixed $0D + 1D$-mix-SnO_2 sample, zero-dimensional sample is characterized by the presence of hysteresis and significantly lower values of current—up to 6 nA compared with 0–0.004 μA for the sample $0D + 1D$-mix SnO_2. Modifying the $0D$-SnO_2 sample with argentum leads to the hysteresis decreasing and, in the case of samples modified with argentum in the amount of 2% and 5%, to increasing the current values up to 2.2 μA and 90 μA, respectively. For the $0D$-10AgSnO_2 sample, the values of the current flowing through the substrate is in the range 0–3000 nA. The addition of argentum in the amount of 10% causes a significant decrease in the values of current strength. In the case of modified

TABLE 2. Electrical properties of tin(IV)-oxide powders at ambient and potential 2.5 V.

Sample	Current, μA	Resistance, MOhm	Conductance, μS
$0D$-SnO_2	0.002	1296.00	0.001
$0D + 1D$-mix SnO_2	0.001	1782.00	0.001
$0D$-2$AgSnO_2$	0.882	2.84	0.352
$0D$-5$AgSnO_2$	0.976	2.56	0.391
$0D$-10$AgSnO_2$	1.625	1.54	0.649
$0D + 1D$-mix 2$AgSnO_2$	0.042	59.43	0.017
$0D + 1D$-mix 5$AgSnO_2$	0.031	80.90	0.012
$0D + 1D$-mix 10$AgSnO_2$	0.039	63.83	0.016

mixed SnO_2 samples, the hysteresis appears and the current decreases to values of 60–100 nA.

Differences in the volt–ampere curves of the synthesized samples are due to the difference in the morphology of $0D$- and $1D$-SnO_2 nanostructures. It is known that the sharper graph goes to the top, the greater conductivity of the sensitive layer and, as a result, the greater response of gas sensor will be. The lack of hysteresis on the I–U curves is more desirable, because of better stability of devices' work characteristics in this case.

Based on the data of the volt–ampere dependences at the same value of potential, the electrical characteristics of the studied samples were calculated (Table 2).

$0D$- and mixed $0D + 1D$-tin(IV)-oxide samples differed slightly in their values of current and, as a result, exhibited equal conductance. It can also be seen that for mixed zero- and one-dimensional SnO_2 samples modified with different amounts of Ag, the conductivity values lie in the almost one range and pass through the maximum. Moreover, in the case of $0D$-SnO_2 nanostructures, the conductivity increases with increasing of Ag content.

3.4. Temperature Influence on Electric Characteristics

Sensors used to analyze gaseous substances usually operate at elevated temperatures. Therefore, it is important to know the dependence of electrical conductivity of the investigated samples on temperature. Electrodes with deposited on them powders were investigated when heated from 303 K to 423 K and with appropriate cooling. The measurement of the resistance data was performed at 2.5 V.

The dependences of electrical conductivity on temperature when

heating and cooling are presented in Fig. 4.

For all studied samples, there is a general tendency—their conductivity increases with the temperature increasing. The value of conductivity during heating at the same temperature is lower than during cooling. The $0D$-SnO_2 sample was characterized by conductivity values 10 times higher than those for the mixed $0D + 1D$-mix-SnO_2 sample were. Modifying of the zero-dimensional powder with 2% Ag leads to the significant growth in conductivity, however further increase in the argentum content causes decreasing of the

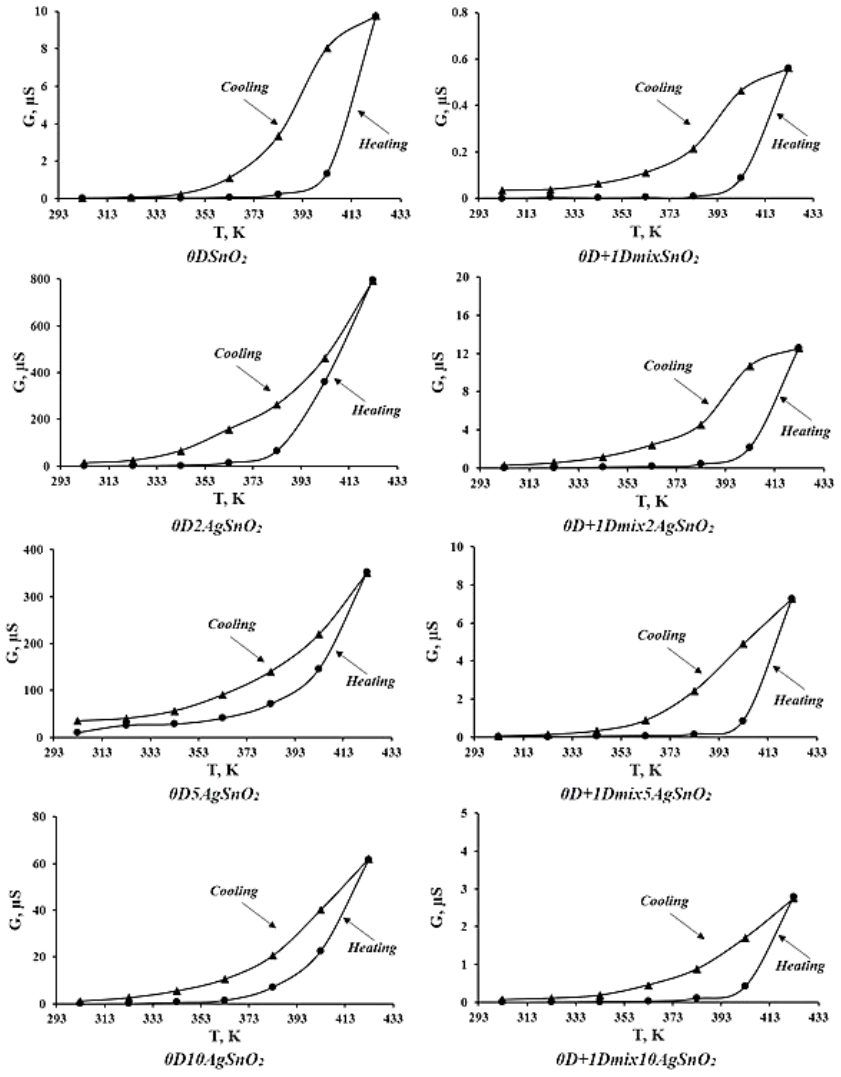

Fig. 4. Dependence of electrical conductivity on temperature of SnO_2 samples.

electrical conductivity. Similar data is obtained in the case of the sample represented by the mixture of 0*D*- and 1*D*-SnO_2 nanostructures. Adding Ag in this case negatively affected the electrical properties of powders.

3.5. Chronoamperometry

Analysis of chronoamperograms was carried out using the program 'Chronoamperometry' [41]. This program is intended for recording

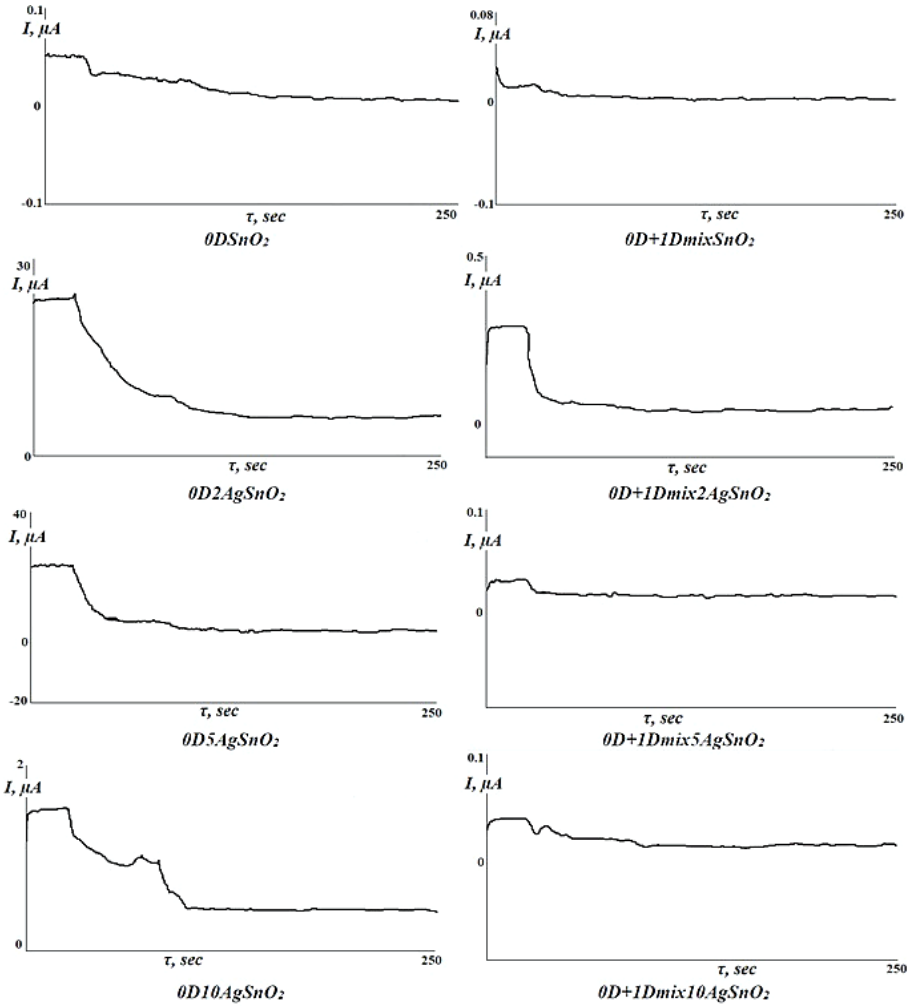

Fig. 5. Chronoamperograms of SnO_2 samples under the influence of ethyl acetate.

current with the established voltage between electrodes. It allowed setting of the measuring period, the range of current in the graphic field, the level of noise dumping. The program was used to study photoelectric effects and changes in powder parameters under the influence of studied substances vapours. It was assumed that, for practical application, value of the voltage applied to the electrodes would normally not exceed half the typical voltage of the microprocessor controllers' supply, which is equal to 2.5 V. Therefore, the resistance analysis of the electrodes coated with the investigated powders was carried out at 2.5 V.

Figures 5 and 6 show chronoamperograms of the synthesized pure and modified tin(IV)-oxide samples of different morphology under the influence of ethyl acetate and chlorobenzene vapours.

Modification of zero-dimensional tin(IV)-oxide sample with argentum in the amount of 2% and 5% leads to the improved response of the sensitive layer to ethyl acetate and chlorobenzene compared with pure $0D$-SnO_2. When increasing the content of argentum to 10%, there is a decrease in sensitivity of the modified zero-dimensional tin(IV)-oxide sample both to the ethyl acetate and chlorobenzene vapours.

Accordingly to the obtained amperograms, for the modified mixed zero- and one-dimensional samples, it can be concluded that, in the case of ethyl acetate detection, adding argentum has a rather negative impact (Fig. 5). However, presented results show that sensitivity of the mixed SnO_2 sample to chlorobenzene can be improved by its modification with argentums; especially, it is noticeable for the $0D + 1D$-mix-2AgSnO_2 sample (Fig. 6).

3.6. Sensitivity

Sensitivity of the SnO_2 films to ethyl acetate and chlorobenzene vapours was calculated on the basis of processing data obtained from chronoamperograms, taking into account resistance values of the sensitive film at ambient and resistance values under the influence of vapours [31]. The results of the calculations are given in Tables 3 and 4.

From the obtained data, it can be seen that both unmodified samples show good sensitivity to ethyl acetate vapours. Significantly lower response was obtained for chlorobenzene—21% and 0.5% for zero-dimensional and mixed samples, respectively.

Among modified zero-dimensional samples, the best response to ethyl acetate vapours was observed for powders modified with 2% and 5% of argentum. Modification of $0D + 1D$-mix-SnO_2 sample with 2% Ag slightly increased sensitivity to ethyl acetate and increasing of argentum content led to the sensory response decreas-

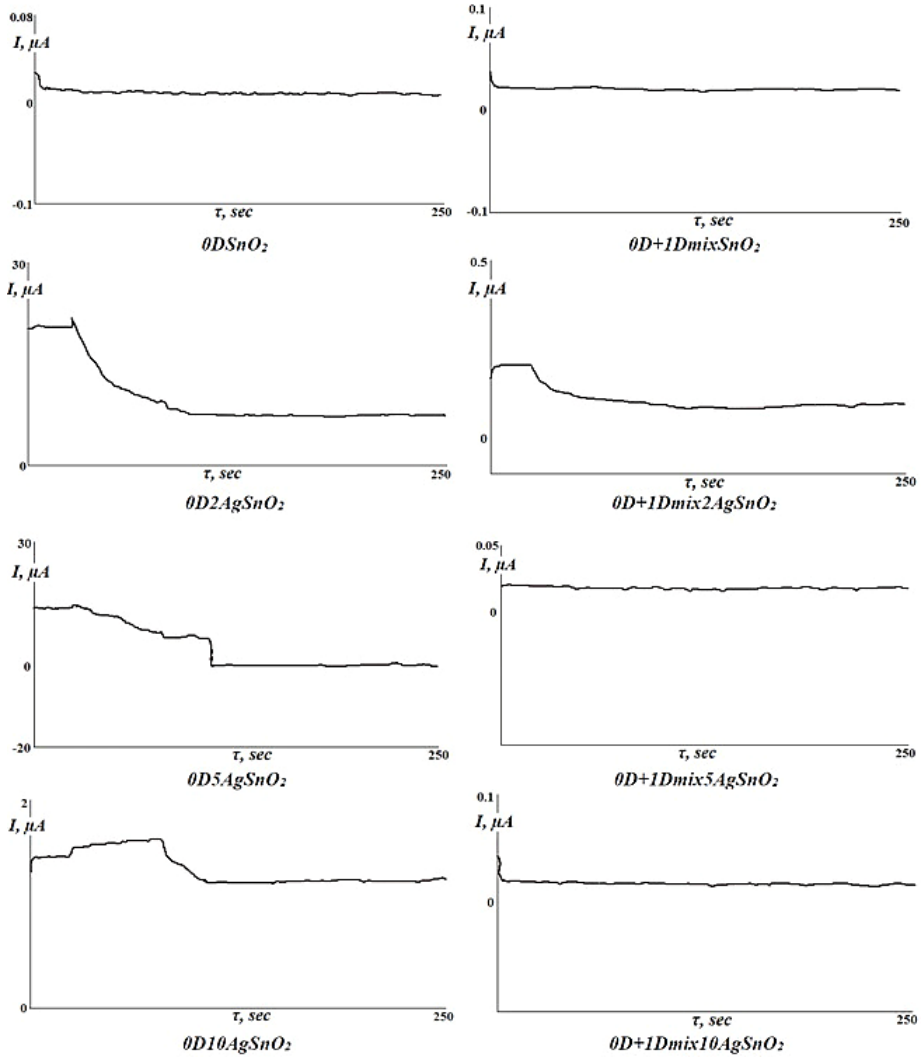

Fig. 6. Chronoamperograms of SnO_2 samples under the influence of chlorobenzene.

ing. It is worth noting that when increasing the percentage of argentum to 10%, the sensitivity of tin(IV)-oxide samples to ethyl acetate deteriorates sharply. In the case of chlorobenzene detection, modification with argentum showed strong sensitivity improvement that is especially noticeable for SnO_2 samples modified with 2% Ag.

In our opinion, the different influence of argentum on the sensitivity of $0D$- and $0D + 1D$-tin(IV)-oxide samples is related to the barrier conductivity of these samples, the main parameter of which

TABLE 3. Sensitivity of SnO_2 samples to ethyl acetate at 303 K.

Sample	Parameters before gas passing		Parameters after gas passing		S, %
	I, μA	R, MOhm	I, μA	R, MOhm	
$0D$-SnO_2	0.050	49.702	0.024	103.734	109
$0D + 1D$-mix SnO_2	0.015	166.667	0.003	827.815	397
$0D$-2$AgSnO_2$	24.580	0.102	9.570	0.261	157
$0D$-5$AgSnO_2$	23.720	0.105	6.860	0.364	246
$0D$-10$AgSnO_2$	1.500	1.666	0.920	2.714	63
$0D + 1D$-mix 2$AgSnO_2$	0.285	8.766	0.056	44.964	413
$0D + 1D$-mix5$AgSnO_2$	0.031	79.847	0.017	147.929	85
$0D + 1D$-mix 10$AgSnO_2$	0.039	64.218	0.020	126.775	97

TABLE 4. Sensitivity of SnO_2 samples to chlorobenzene at 303 K.

Sample	Parameters before gas passing		Parameters after gas passing		S, %
	I, μA	R, MOhm	I, μA	R, MOhm	
$0D$-SnO_2	0.014	185.736	0.011	225.225	21
$0D + 1D$-mix SnO_2	0.021	117.371	0,021	117.925	0.5
$0D$-2$AgSnO_2$	20.530	0.122	9.560	0.262	115
$0D$-5$AgSnO_2$	13.830	0.181	7,870	0.318	76
$0D$-10$AgSnO_2$	1.450	1.725	1.600	1.563	9
$0D + 1D$-mix 2$AgSnO_2$	0.201	12.413	0.104	23.969	93
$0D + 1D$-mix 5$AgSnO_2$	0.020	126.711	0.018	136.314	8
$0D + 1D$-mix 10$AgSnO_2$	0.021	118.483	0.019	133.690	13

is the height of barriers at the nanoparticles' boundary. For unmodified powders, in the case of nanosize SnO_2, the number of barriers is larger than for mixed SnO_2 structures. When doping $0D$-tin(IV)-oxide powders, argentum first increases and then reduces the height of the barriers, the charge transfer is facilitated, respectively, the electrical conductivity increases. For the mixed zero- and one-dimensional structures, the unmodified sample is characterized by a significantly smaller number of energy barriers, adding the argentum causes their formation, which worsens electrical conductivity.

4. CONCLUSIONS

SnO_2 nanostructures of different morphology (zero-dimensional and

mixed zero- and one-dimensional) were synthesized *via* the chemical vapour deposition method. Obtained samples were modified with argentum in the amount of 2%, 5% and 10% by impregnating method. The sensitivity zero-dimensional and mixed zero- and one-dimensional SnO_2 nanostructures obtained by CVD method towards ethyl acetate and chlorobenzene vapours was first determined.

The current–voltage dependences of pure and modified SnO_2 samples are characteristic of materials with semiconducting properties. The investigation of synthesized tin(IV)-oxide powders using the chronoamperometry method showed that in most cases SnO_2 had the good reaction to ethyl acetate, which is associated with higher values of the specific electrical conductivity of these substances. Both pure tin(IV)-oxide samples show good sensitivity to ethyl acetate and much worse reaction to chlorobenzene vapours. Among the modified samples, the best response to vapours of organic compounds was observed for powders modified with 2% and 5% of Argentum.

The effect of the modifier is ambiguous, depending on the morphology of SnO_2; modification of zero-dimensional tin(IV)-oxide structures leads to improved electrical characteristics and sensitivity of the synthesized samples; while adding argentum to the mixed zero- and one-dimensional nanostructures in most cases has a negative effect. This can be explained by different barrier conductivity of these samples, which relates to their morphology. Thus, in this case, morphology has bigger influence on sensitivity than modification.

REFERENCES

1. P. Harb, N. Locoge, and F. Thevenet, *Chemical Engineering Journal*, **354**: 641 (2018); https://doi.org/10.1016/j.cej.2018.08.085
2. W. Wei, Z. F. Lv, Y. Li, L. T. Wang, S. Cheng, and H. Liu, *Atmospheric Environment*, **175**: 44 (2018); https://doi.org/10.1016/j.atmosenv.2017.11.058
3. R. Hu, G. Liu, H. Zhang, H. Xue, and X. Wang, *Ecotoxicology and Environmental Safety*, **160**: 301 (2018); https://doi.org/10.1016/j.ecoenv.2018.05.056
4. S. Korgaokar, M. Moradiya, O. Prajapati, P. Thakkar et al., *Functional Oxides and Nanomaterials*, **1837**: 1 (2017); https://doi.org/10.1063/1.4982134
5. P. Kumar, A. Deep, K.-H. Kim, and R. J. C. Brown, *Progress in Polymer Science*, **45**: 102 (2015); https://doi.org/10.1016/j.progpolymsci.2015.01.002
6. *U.S. National Library of Medicines* https://pubchem.ncbi.nlm.nih.gov/compound/ethyl_acetate
7. *U.S. National Library of Medicines* https://pubchem.ncbi.nlm.nih.gov/compound/chlorobenzene

8. S. K. Jha, R. D. S. Yadava, K. Hayashi, and N. Patel, *Chemometrics and Intelligent Laboratory Systems*, **185**: 18 (2019); https://doi.org/10.1016/j.chemolab.2018.12.008
9. Z. Bielecki, T. Stacewicz, J. Wojtas, J. Mikołajczyk, D. Szabra, and A. Prokopiuk, *Opto-Electronics Review*, **26**, No. 2: 122 (2018); https://doi.org/10.1016/j.opelre.2018.02.007
10. A. Mirzaei, S. G. Leonardi, and G. Neri, *Ceramics International*, **42**, No. 14: 15119 (2016); https://doi.org/10.1016/j.ceramint.2016.06.145
11. X. Zhou, J. Liu, C. Wang, P. Sun, X. Hu, X. Li, and G. Lu, *Sensors and Actuators B: Chemical*, **206**: 577 (2015); https://doi.org/10.1016/j.snb.2014.09.080
12. T. A. Dontsova, S. V. Nahirniak, and I. M. Astrelin, *Journal of Nanomaterials*, **2019**: 1 (2019); https://doi.org/10.1155/2019/5942194
13. G. Korotcenkov and B. K. Cho, *Sensors and Actuators B: Chemical*, **244**: 182 (2017); https://doi.org/10.1016/j.snb.2016.12.117
14. M. Arafat, B. Dinan, S. A. Akbar, and A. Haseeb, *Sensors*, **12**: 7207 (2012); https://doi.org/10.3390/s120607207
15. M. Al-Hashem, S. Akbar, and P. Morris, *Sensors and Actuators B: Chemical*, **301**: 126845 (2019); https://doi.org/10.1016/j.snb.2019.126845
16. A. Sviderskyi, S. Nahirniak, T. Yashchenko, T. Dontsova, and S. Kalinowski, *2018 IEEE 8th International Conference 'Nanomaterials: Applications & Properties (NAP)'* (IEEE: 2018), p. 1; https://doi.org/10.1109/NAP.2018.8914913
17. S. Nahirniak, T. Dontsova, and I. Astrelin, *Nanochemistry, Boitechnology, Nanomaterials, and Their Applications*, **214**: 233 (2018); https://doi.org/10.1007/978-3-319-92567-7_14
18. T. Munawar, F. Iqbal, S. Yasmeen, K. Mahmood, and A. Hussain, *Ceramics International*, **46**, Iss. 2: 2421 (2020); https://doi.org/10.1016/j.ceramint.2019.09.236
19. Y. I. Venhryn, S. S. Savka, R. V. Bovhyra, V. M. Zhyrovetsky, A. S. Serednytski, and D. I. Popovych, *Materials Today: Proceedings*, **35**, Pt. 4: 588 (2019); https://doi.org/10.1016/j.matpr.2019.11.118
20. C. M. Hung, D. T. T. Le, and N. Van Hieu, *Journal of Science: Advanced Materials and Devices*, **2**, No. 3: 263 (2017); https://doi.org/10.1016/j.jsamd.2017.07.009
21. H.-J. Kim and J.-H. Lee, *Sensors and Actuators B: Chemical*, **192**: 607 (2014); https://doi.org/10.1016/j.snb.2013.11.005
22. A. Moezzi, A. M. McDonagh, and M. B. Cortie, *Chemical Engineering Journal*, **185–186**: 1 (2012); https://doi.org/10.1016/j.cej.2012.01.076
23. H. Wang, Y. Qu, H. Chen, Z. Lin, and K. Dai, *Sensors and Actuators B: Chemical*, **201**: 153 (2014); https://doi.org/10.1016/j.snb.2014.04.049
24. G. Fedorenko, L. Oleksenko, N. Maksymovych, G. Skolyar, and O. Ripko, *Nanoscale Research Letters*, **12**: 329: 1 (2017); https://doi.org/10.1186/s11671-017-2102-0
25. S. Das and V. Jayaraman, *Progress in Materials Science*, **66**: 112 (2014); https://doi.org/10.1016/j.pmatsci.2014.06.003
26. G. Korotcenkov and B. K. Cho, *Sensors and Actuators B: Chemical*, **161**, No. 1: 28 (2012); https://doi.org/10.1016/j.snb.2011.12.003
27. J. P. Cheng, J. Wang, Q. Q. Li, H. G. Liu, and Y. Li, *Journal of Industrial*

and Engineering Chemistry, **44**: 1 (2016); https://doi.org/10.1016/j.jiec.2016.08.008
28. E. B. Aydın and M. K. Sezgintürk, *TrAC Trends in Analytical Chemistry*, **97**: 309 (2017); https://doi.org/10.1016/j.trac.2017.09.021
29. G. Korotcenkov and B. K. Cho, *Sensors and Actuators B: Chemical*, **196**: 80 (2014); https://doi.org/10.1016/j.snb.2014.01.108
30. P. O. Patil, G. R. Pandey, A. G. Patil, V. B. Borse, P. K. Deshmukh, D. R. Patil, R. S. Tade, S. N. Nangare, Z. G. Khan, A. M. Patil, M. P. More, M. Veerapandian, and S. B. Bari, *Biosensors and Bioelectronics*, **139**: 111324 (2019); https://doi.org/10.1016/j.bios.2019.111324
31. S. V. Nahirniak, T. A. Dontsova, and Q. Chen, *Molecular Crystals and Liquid Crystals*, **674**, No. 1: 48 (2019); https://doi.org/10.1080/15421406.2019.1578511
32. G. Adachi and N. Imanaka, *Handbook on the Physics and Chemistry of Rare Earths* (1995), vol. **21**, Ch. 143, p. 179; https://doi.org/10.1016/S0168-1273(05)80112-6
33. V. M. Aroutiounian, V. M. Arakelyan, E. A. Khachaturyan, G. E. Shahnazaryan, M. S. Aleksanyan, L. Forro, and Z. Nemeth, *Sensors and Actuators B: Chemical*, **173**: 890 (2012); https://doi.org/10.1016/j.snb.2012.04.039
34. A. K. Srivastava, *Sensors and Actuators B: Chemical*, **96**, Nos. 1–2: 24 (2003); https://doi.org/10.1016/S0925-4005(03)00477-5
35. L. Song, L. Yang, Z. Wang, D. Liu, L. Luo, X. Zhu, and Y. Chen, *Sensors and Actuators B: Chemical*, **283**: 793 (2019); https://doi.org/10.1016/j.snb.2018.12.097
36. T. A. Dontsova, S. V. Nagirnyak, V. V. Zhorov, and Y. V. Yasiievych, *Nanoscale Research Letters*, **12**: 332: 1 (2017); https://doi.org/10.1186/s11671-017-2100-2
37. S. V. Nagirnyak, V. A. Lutz, T. A. Dontsova, and I. M. Astrelin, *Nanoscale Research Letters*, **11**: 343-1 (2016); https://doi.org/10.1186/s11671-016-1547-x
38. S. Nagirnyak, V. Lutz, T. Dontsova, and I. Astrelin, *Nanophysics, Nanophotonics, Surface Studies, and Applications. Springer Proceedings in Physics* (Eds. O. Fesenko and L. Yatsenko) (Cham: Springer: 2016), vol. **183**, p. 331; https://doi.org/10.1007/978-3-319-30737-4_28
39. S. Nagirnyak and T. Dontsova, *2017 IEEE 7th International Conference 'Nanomaterials: Applications & Properties (NAP)'* (IEEE: 2017), p. 01NNPT13-1; https://doi.org/10.1109/NAP.2017.8190193
40. R. A. Binions and I. P. Parkin, *Mes. Sci. Technol.*, **18**: 190 (2007); https://doi.org/10.1088/0957-0233/18/1/024
41. http://debiany.pl/ksp/
42. G. W. Thomson, *Chemical Reviews*, **38**, No. 1: 1 (1946); https://doi.org/10.1021/cr60119a001